DISTRIBUTION OF PLAGIOCLASE-RICH MATERIALS IN THE LUNAR HIGHLANDS AS INFERRED FROM LUNAR PROSPECTOR THERMAL NEUTRON MEASUREMENTS. P. N. Peplowski[1*], A. W. Beck[1], and D. J. Lawrence[1], [1]The Johns Hopkins University Applied Physics Laboratory, 11100 Johns Hopkins Road, Laurel MD 20723 USA, [*]Patrick.Peplowski@jhuapl.edu

Introduction: New remote sensing observations of the lunar surface [1-5] and detailed chemical studies of feldspathic lunar meteorites (FLMs; [6-7]) are reshaping our view of the chemical and mineralogical composition of the feldspathic highlands terrane (FHT; [8]). This information helps decipher the evolution of the Moon's primordial crust, as the FHT is generally accepted to be the modified remains of a primitive, plagioclase-rich anorthositic floatation crust resulting from the evolution of a global magma ocean (GMO). Recent detections of nearly pure anorthosite (PAN) [1,3-5] support this view, however data revealing a predominance of magnesian, not ferroan, anorthosites [2,7] is inconsistent with simple GMO models [9].

We present a new analysis of Lunar Prospector (LP) Neutron Spectrometer (NS) thermal neutron maps. We use the thermal neutron data to produce a quantity directly linked with bulk chemical composition, which we subsequently use to infer plagioclase concentrations in the lunar highlands. The data provide a near-global view of plagioclase concentrations that complements localized PAN detections.

Thermal Neutron Maps: Our analysis begins with the LP/NS thermal neutron maps, a PDS-archived product produced following the methodology of *Maurice et al.* [10]. The thermal neutron count rates vary appreciably over the surface, including a ~30% variability across the lunar highlands (Figure 1A). Thermal neutron count rates are inversely proportional to the bulk concentrations of neutron absorbing elements, which on the Moon includes Fe, Ti, and Rare Earth Elements (REEs) like Gd and Sm [11].

Geochemical Composition: We convert thermal neutron count rates to the macroscopic neutron absorption cross section (Σ_a), a bulk geochemical parameter that is the weighted sum of the individual microscopic neutron absorption cross sections for each elemental constituent of the lunar surface (e.g. [11]). The conversion is based on a comparison of LP/NS measurements over the Apollo and Luna sample sites to the expected thermal neutron properties of the respective samples. Modeled thermal neutron count rates for materials with highlands-like compositions, derived from measured chemical compositions of 22 Feldspathic Lunar Meteorites (FLMs; taken from [12]), were used to examine the behavior of thermal neutrons the low absorption (low Fe, Ti, and REE) regions. Our Σ_a map is shown in Figure 1B.

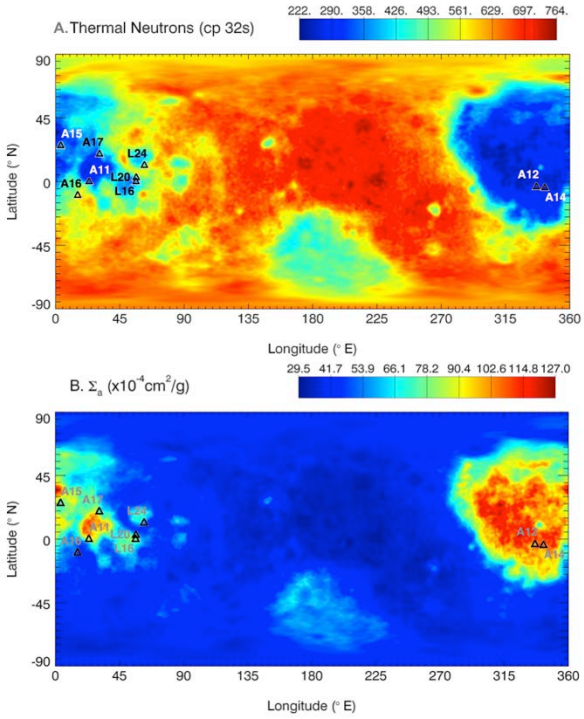

Figure 1. A. LP/NS Thermal neutron map. B. Σ_a map.

Plagioclase Concentrations from Σ_a. FLMs provide a useful reference for investigating the link between Σ_a values and bulk plagioclase content. The relationship is indirect, and stems from the fact that the elemental constituents of plagioclase have low microscopic neutron absorption properties. We begin by calculating Σ_a values and plagioclase concentrations for each FLM. Plagioclase is derived by attributing all Al within the FLM to Ca-rich plagioclase, an assumption based on the fact that it is the major Al-bearing mineral in Fe-poor lunar materials. The FLMs reveal an inverse linear relationship between Σ_a and Al-estimated plagioclase content (Fig. 2). Because this relationship was derived for low-absorption (low Fe, Ti, and REE) material, its use is restricted to the lunar highlands to avoid contamination by REE-bearing KREEP and Fe- and/or Ti-rich mare basalts, which also have Al-bearing phases other than plagioclase. Deviations from our assumed mineralogy (e.g. small contributions from Na-bearing plagioclase) and the spread of values in Figure 2 suggest an ~10% uncertainty in plagioclase concentrations estimated from Figure 2.

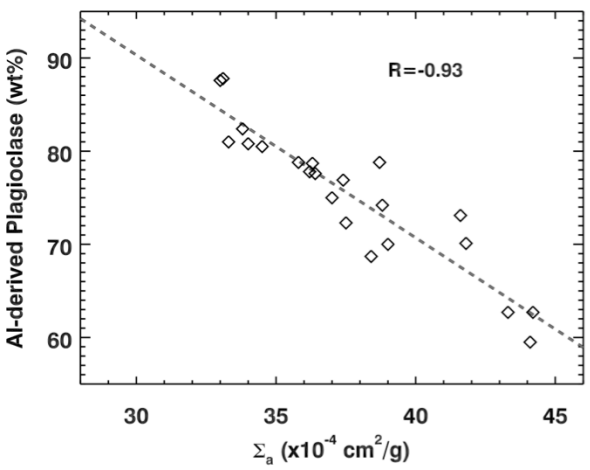

Figure 2. Relationship between plagioclase concentration (derived from Al abundance) and Σ_a for the 22 feldspathic lunar meteorites used in this study.

The validity of Σ_a-derived plagioclase concentrations is supported by: 1) A strong inverse correlation between Σ_a and lunar albedo, 2) a spatial correlation between regions of low Σ_a (>85 wt%) plagioclase and PAN deposits observed by Kaguya and M3 [1,3-5], see Fig. 3, and 3) a general similarity to plagioclase concentrations derived from Clementine UVVS data [13].

Discussion: PAN detections are limited to fresh (not space weathered) materials with high (> ~95 v%) plagioclase content [1,3-5]. The LP/NS measurements are not hindered by these requirements, and provide a near-global, ~45-km resolution view that compliments PAN identifications. LP/NS data reveal extensive regions of low Σ_a (and by inference high, >85 wt% plagioclase) content associated with the FHT [8]. The association of low Σ_a values with impact basins (Fig. 3) supports the presence of a subsurface PAN-bearing layer [1,3-5]. The heterogeneous distribution of plagioclase-rich materials indicates that processes other than simple cumulate floatation played major roles in lunar crustal formation. This could include heterogeneous GMO or mantle, cumulate overturn within the GMO (e.g. [14]), post-GMO serial magmatism [7, 14], and/or asymmetric crustal growth [2, 15].

References: [1] Ohtake, M., et al. (2009) *Nature, 41,* 236-240. [2] Ohtake, M., et al. (2012) *Nat. Geosci., 5,* 384-388. [3] Yamamoto, S. et al. (2012), GRL 39, L13201. [4] Cheek, L.C. et al. (2013) *JGR, 118,* 1805-1820. [5] Donaldson Hanna, K.L. et al. (2014) *JGR, 119,* 1516-1545. [6] Borg, L.E. et al. (2011) *Nature, 447,* 70-73. [7] Gross, J. et al. (2014) *EPSL, 388,* 318-328. [8] Joliff, B. et al. (2000), *JGR 105*, 4197-4216. [9] Wood, J.A. et al. (1970) *Proc. Apollo 11 Lunar Sci. Conf.,* 965-988. [10] Maurice, S. et al. (2004) *JGR, 109,* 1665-1679. [11] Elphic, R.C. et al. (2000) *JGR, 105,* E001176. [12] Calzada-Diaz, A., et al. (2015) *MAPS, 50,* 214-228. [13] Crites, S. and Lucey, P.G. (2015), *Amer. Mineral. 100*, 973-982. [14] Elkins-Tanton, L.T. et al. (2011) *EPSL, 304,* 326-336. [13] Walker, D. (1983) *JGR, 88,* B17-B25. [15] Longhi, J. and Ashwal, L.D. (1985), *JGR, 90,* C571-C584.

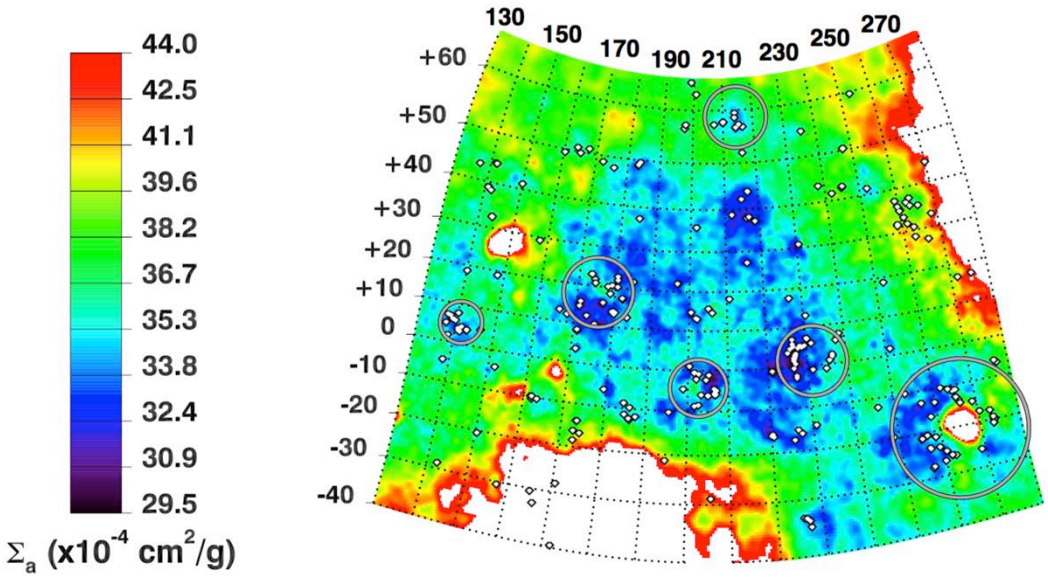

Figure 3. Σ_a map, with locations of nearly pure anorthosite as identified with Kaguya [3] or M3 [5] shown as white diamonds. Σ_a values of <34x10^{-4} cm^2/g correspond to estimated plagioclase concentrations of >85 wt% (±10%). Large basins that appear to be associated with the highest plagioclase concentrations are shown as grey outlines, left to right: Orientale, Hertzsprung, Birkoff, Korolev, Freundlich-Sharonov, Mendeleev.